·论 著·

MRI鉴别宫颈腺体叶状增生与宫颈胃型腺癌的价值

马凤华[1]，姜安绮[2,3]，陈奕清[2]，徐丛剑[2,3]，康 玉[2,3]

1. 复旦大学附属妇产科医院放射科，上海 200011；
2. 复旦大学附属妇产科医院妇科，上海 200011；
3. 上海市女性生殖内分泌相关疾病重点实验室，上海 200011

［**摘要**］ **背景与目的：**宫颈胃型腺癌（gastric-type endocervical adenocarcinoma，G-EAC）是一种少见的宫颈腺癌，临床表现不典型，病灶隐匿，极易漏诊、误诊，患者预后差；而宫颈腺体叶状增生（lobular endocervical glandular hyperplasia，LEGH）及非典型LEGH（atypical lobular endocervical glandular hyperplasia，aLEGH）是G-EAC的癌前病变，与G-EAC存在临床、病理学及影像学等诸多重叠，术前诊断极具挑战性。本文旨在分析宫颈囊实性病变的磁共振成像（magnetic resonance imaging，MRI）表现与病理学诊断结果的相关性，以提高LEGH与G-EAC鉴别诊断的准确性。**方法：**收集2016年7月—2023年8月在复旦大学附属妇产科医院就诊的37例LEGH和53例G-EAC患者的临床、影像学及病理学资料。采用χ^2检验或Fisher精确概率法等进行统计学分析，采用logistic回归进行多因素分析，采用受试者工作特征（receiver operator characteristic，ROC）曲线进行效能评价。**结果：**LEGH和G-EAC两组间患者年龄、症状、病灶范围、大小、成分、强化程度、宫颈间质环、子宫内膜累及、淋巴结肿大、宫腔积液差异有统计学意义（$P<0.05$）。LEGH及aLEGH组病灶位于宫颈黏膜层，主要表现为大、微小囊混合型或密集微小囊型（32/37），囊壁多明显强化（31/37）；而G-EAC组中多累及宫颈肌层（42/53），多见实性成分（52/53）和低信号间质环中断或消失（46/53）。Logistic回归分析结果显示，病灶实性成分（OR=50.064）和宫颈间质环中断（OR=40.180）可作为预测G-EAC的显著MRI特征。综合病灶大小、成分、强化程度、宫颈间质环和子宫内膜累及5个特征，对诊断G-EAC的效能采用ROC分析，曲线下面积（area under curve，AUC）为0.970（95% CI：0.931～1.008）。**结论：**结合宫颈囊实性病变的多个MRI征象有助于鉴别LEGH与G-EAC。

［**关键词**］宫颈腺体叶状增生；宫颈胃型腺癌；癌前病变；磁共振成像；鉴别诊断

中图分类号：R737.33 **文献标志码：**A DOI: 10.19401/j.cnki.1007-3639.2024.04.005

Magnetic resonance imaging for distinguishing gastric-type endocervical adenocarcinoma from lobular endocervical glandular hyperplasia

MA Fenghua[1], JIANG Anqi[2,3], CHEN Yiqing[2], XU Congjian[2,3], KANG Yu[2,3] (1. Department of Radiology, Obstetrics and Gynecology Hospital, Fudan University, Shanghai 200011, China; 2. Department of Gynecology, Obstetrics and Gynecology Hospital, Fudan University, Shanghai 200011, China; 3. Shanghai Key Laboratory of Female Reproductive Endocrine Related Diseases, Shanghai 200011, China)

Correspondence to: KANG Yu, E-mail: ykang@126.com; XU Congjian, E-mail: xucongjian@fudan.edu.cn

［**Abstract**］ **Background and purpose:** Gastric-type endocervical adenocarcinoma (G-EAC) is a rare variant of endocervical adenocarcinoma, characterized by atypical clinical manifestations and elusive lesions. Due to these factors, G-EAC is prone to being missed or misdiagnosed, significantly impacting the prognosis. Lobular endocervical glandular hyperplasia (LEGH) and atypical LEGH (aLEGH) are considered to be precancerous lesions of G-EAC. These conditions also present overlapping clinical, pathologic and imaging manifestations, making it challenging to differentiate between them preoperatively. The purpose of this study was to investigate the correlation between magnetic resonance imaging (MRI) findings of cystic-solid lesions in the cervix and their

第一作者：马凤华（ORCID: 0000-0002-6486-8058），博士，副主任医师，E-mail: mafenghua9602@163.com；姜安绮（ORCID: 0009-0004-8954-2435），博士研究生在读，E-mail：jaq0413@163.com。马凤华和姜安绮为共同第一作者。
通信作者：康玉（ORCID: 0000-0003-1197-4727），博士，主任医师，E-mail: ykang@126.com；徐丛剑（ORCID: 0000-0002-7954-5832），博士，主任医师，E-mail: xucongjian@fudan.edu.cn。

underlying pathology in order to enhance the accuracy of distinguishing between LEGH and G-EAC, ultimately aiding in the early diagnosis and appropriate management of these conditions. **Methods:** Clinical, imaging and pathological data of 37 LEGH and 53 G-EAC patients who attended the Obstetrics and Gynecology Hospital of Fudan University from July 2016 to August 2023 were collected. Analysis was conducted using Pearson Chi-square χ^2, Fisher's exact tests and so on. Multivariate analyses were performed using logistic regression. Receiver operating characteristic (ROC) curves were used for performance evaluation. **Results:** In this study, differences in age, symptoms, extent, size, composition, degree of enhancement, cervical stromal ring, endometrium invasion, pelvic lymph nodes enlargement, and hydrohystera were statistically significant between the two groups ($P<0.05$). In the LEGH and aLEGH groups, lesions were primarily localized to the epithelial layer of the endocervical canal. These lesions were predominantly simple cystic (32/37), and the cystic walls often displayed significant enhancement (31/37). In contrast, the G-EAC group presented with lesions involving the myometrium of the uterine cervix (42/53). These lesions were characterized by a solid component in the majority of cases (52/53), a tendency for the disappearance of the cervical stromal ring (46/53). Logistic regression analysis revealed that among the MRI features, lesion composition (OR=50.064) and incomplete cervical stromal ring (OR=40.180) were significant predictors for G-EAC. ROC analysis, incorporating lesion size, composition, enhancement degree, cervical stromal ring, and endometrial involvement, yielded an area under curve (AUC) of 0.970 (95% CI: 0.931-1.008). **Conclusion:** Combining multiple MRI features of cystic-solid lesions in the cervix aids in distinguishing between LEGH and G-EAC.

［**Key words**］ Lobular endocervical glandular hyperplasia; Gastric-type endocervical adenocarcinoma; Precancerous lesions; Magnetic resonance imaging; Differential diagnosis

宫颈腺体叶状增生（lobular endocervical glandular hyperplasia，LEGH）形态学表现为宫颈多发囊肿，最初被报道为一种良性增生性疾病[1]；而根据现有研究[2]，LEGH和非典型LEGH（atypical lobular endocervical glandular hyperplasia，aLEGH）可能发展为宫颈胃型腺癌（gastric-type endocervical adenocarcinoma，G-EAC），遂被视为癌前病变。LEGH与G-EAC有许多共同的临床、病理学及影像学特征。临床上，LEGH或G-EAC患者均可表现为阴道分泌物增多，但G-EAC具有更强的侵袭性特征，包括腹膜扩散和较差的预后，且易被漏诊或误诊，患者确诊时往往已处于进展期[3]；病理学表现上，LEGH有一个独特的胃表型（幽门腺化生），HIK1083免疫组织化学检测结果为阳性，G-EAC也表现出独特的幽门化生，HIK1083免疫组织化学检测结果呈阳性，高达20%的G-EAC可合并LEGH[2]；影像学上，LEGH和G-EAC均可表现为多房性囊性肿块[1]。因此，早期鉴别G-EAC与LEGH并予以相称的术前诊断对后续的临床决策十分重要。

磁共振成像（magnetic resonance imaging，MRI）具有良好的软组织对比及多方位成像的优势，在显示宫颈解剖及疾病方面较超声和计算机体层成像（computed tomography，CT）更准确、更特异[4]。目前影像学研究[5-6]结果显示，LEGH主要表现为多囊性病灶，而G-EAC主要表现为囊实性病灶，两者的MRI特征仍有诸多重叠，且对于宫颈多囊性病变的影像学诊断尚缺乏统一标准。宫颈多囊性病变的临床决策与术前诊断结果息息相关，当MRI提示病灶明显具有G-EAC的恶性征象时，建议通过活组织检查获取病理学证据[6]。若检查结果提示为LEGH，可结合患者的年龄和生育状况，采用MRI明确病变累及的范围及采用宫颈细胞学检查等密切随访，避免过度治疗[7]。因此，本研究拟探究LEGH和G-EAC的MRI特征并对二者进行统计学分析，旨在提高MRI鉴别诊断二者的准确性，为临床治疗提供依据。

1 资料和方法

1.1 一般资料

收集2016年7月—2023年8月在复旦大学附属妇产科医院就诊的37例LEGH和53例G-EAC患者的临床、影像学及病理学资料。入组标准：① 患者在本院接受了MRI检查，影像资料清晰且齐全；② 患者在本院接受活检、手术或病理学会

诊，经病理学检查证实为LEGH或aLEGH或浸润性G-EAC。排除标准：① 临床、影像学或病理学资料不完整；② 病理学检查时取材不完整，更重病变不能排除。临床资料包括患者的年龄、症状、活检或手术方式；影像学资料包括病灶范围、大小、成分、增强程度、宫颈间质环和伴发征象（子宫是否累及、卵巢是否有病变、淋巴结有无增大、宫腔积液和膀胱侵犯）；病理学资料包括病灶位置、大体病理学特征等。

1.2 检查方法

采用1.5T MR超导扫描仪（Symphony或Avanto, Siemens）或3.0T MR超导扫描仪（Ingenia 3.0T, Philips），相控阵体线圈。患者仰卧，自由呼吸。1.5T扫描参数及序列如下：先行快速自旋回波序列（fast spin echo sequence，FSE）平扫，矢状位T2加权（T2WI）抑脂，重复时间/回波时间（time of repetition/time of echo，TR/TE）为4 000/83 ms；横断位T1加权（T1WI），TR/TE为761 ms/10 ms；横断位T2WI抑脂，TR/TE为8 000 ms/83 ms；冠状位T2WI抑脂，TR/TE为4 000 ms/98 ms；视野（field of vision，FOV）为（300～380）mm×（320～400）mm；矩阵为256×256或320×320；层厚/层距为（4.0～8.0）mm/（1.2～1.5）mm；激励次数为4次。3.0T扫描参数及序列如下：先行频率衰减反转恢复序列（spectral attenuated inversion recovery，SPAIR）平扫，矢状位T2WI抑脂，TR/TE为3 223/100 ms；横断位涡轮自旋回波序列（turbo spin echo sequence，TSE）T1WI，TR/TE为400/18 ms；横断位SPAIR T2WI抑脂，TR/TE为2 723/100 ms；冠状位TSE T2WI，TR/TE为2 000/80 ms；FOV为（300～380）mm×（320～400）mm；矩阵为256×256或320×320；层厚/层距为（4.0～6.0）mm/（-1.2～0）mm；激励次数为1~2次。增强对比剂为钆喷替酸葡甲胺（0.2 mmol/kg，2～3 mL/s），横断位、冠状位、矢状位T1WI扫描，参数同平扫。

1.3 图像分析

由2名具有腹部影像诊断经验10年以上的医师分别对MRI结果进行分析，对患者的病理学诊断采用盲法，意见不同时协商达成一致，内容包括：① 病灶范围（宫颈管黏膜层或黏膜肌层是否均有病变）；② 病灶大小，包括宫颈横断位、矢状位及冠状位的最大径线；③ 囊性结构分类，包括微小囊（囊腔直径≤5 mm）和大囊（囊腔直径＞5 mm）；④ 病灶成分，包括大小囊混合型（无实性区，大囊、微小囊混合分布，微小囊≤2/3）、微小囊型（以微小囊为主，可有少许实性区，微小囊＞2/3）、囊实性混合型（实性和囊性区交织分布，实性区≤2/3）或实性为主型（实性区＞2/3，局部偶可见囊性灶）；⑤ 病灶强化程度，包括轻中度（弱于子宫肌层）或明显强化（接近或强于子宫肌层）；⑥ 宫颈T2WI低信号间质环，包括连续或中断、消失；⑦ 伴发异常，包括卵巢有无病变、子宫内膜或肌层有无累及、淋巴结有无增大、宫腔有无积液和膀胱或直肠有无侵犯等。

1.4 统计学处理

采用Pearson Chi-square χ^2检验或Fisher精确概率法比较LEGH和aLEGH组与G-EAC组的症状、病灶范围、成分、增强程度、宫颈间质环及伴发异常，采用两独立样本的Mann-Whitney Test比较两组间患者的年龄和病灶最大径。采用多因素logistic回归和受试者工作特征（receiver operator characteristic，ROC）曲线分析筛选有助于鉴别两者的影像学特征。P＜0.05为差异有统计学意义。数据分析采用SPSS 26.0软件。

2 结　果

2.1 临床特征

本研究共纳入90例患者。患者年龄为21～79岁，平均年龄（44.0±11.6）岁；其中，16例LEGH和21例aLEGH，患者年龄为21～79岁，平均（41.0±10.5）岁；53例G-EAC，年龄27～73岁，平均（46.0±12.0）岁。临床表现，阴道分泌物增多52例（52/90，57.8%），阴道不规则出血29例（29/90，32.2%），腹痛11例（11/90，12.2%）。LEGH患者无阴道不规则出血和腹痛表现，腹痛表现均见于G-EAC患者。年龄、阴道分

泌物增多、阴道不规则出血和腹痛在两组间差异有统计学意义（$P<0.05$，表1）。

表1 宫颈（不典型）叶状增生与胃型腺癌临床特征的比较

Tab. 1 Comparison of clinical features between (atypical) LEGH and G-EAC

Clinicopathologic characteristics	LEGH+aLEGH (*n*=37)	G-EAC (*n*=53)	*P* value
Mean age/year	41.0±10.5	46.0±12.0	0.015
Manifestations			
Vaginal discharge	31 (83.8%)	21 (39.6%)	<0.001
Vaginal bleeding	2 (5.4%)	27 (50.9%)	<0.001
Abdominal pain	0	11 (20.8%)	0.009

LEGH: Lobular endocervical glandular hyperplasia; aLEGH: Atypical lobular endocervical glandular hyperplasia; G-EAC: Gastric-type endocervical adenocarcinoma.

2.2 影像学特征

经回顾性统计，90例患者的MRI初始诊断结果与病理学检查结果的总体一致率为67.8%（61/90），LEGH及aLEGH组为51.4%（19/37），G-EAC组为79.2%（42/53）。影像学诊断与病理学诊断的一致性结果见表2。

表2 影像学诊断与病理学诊断的一致性

Tab. 2 Concordance between imaging diagnoses and pathology results

Imaging diagnoses	LEGH+aLEGH (*n*=37)	G-EAC (*n*=53)
sLEGH	19 (51.4%)	5 (9.4%)
sMT	5 (13.5%)	42(79.2%)
Non-specific	13 (35.1%)	6 (11.3%)
Consistency rate	51.4%	79.2%

LEGH: Lobular endocervical glandular hyperplasia; aLEGH: Atypical lobular endocervical glandular hyperplasia; G-EAC: Gastric-type endocervical adenocarcinoma; sLEGH: Suspected lobular endocervical glandular hyperplasia; sMT: Suspected malignant tumor.

系统分析LEGH、aLEGH和G-EAC的MRI特征结果见表3。LEGH及aLEGH组病灶局限于宫颈黏膜层，最大径为（3.4±1.1）cm；而G-EAC组中有79.2%（42/53）病灶累及宫颈肌层，且最大径为（4.7±1.6）cm。LEGH及aLEGH组主要表现为大、微小囊混合型或密集微小囊型（32/37，86.5%），仅5例（13.5%）为囊实性混合型，增强扫描后囊壁多为明显强化（31/37，83.8%）；G-EAC病灶多可见实性成分，其中囊实性混合型和实性为主型分别为16例（30.2%）和36例（67.9%），仅1例呈囊性型（1.9%），增强扫描后病灶呈明显强化者31例（58.5%），轻度强化22例（41.5%）。宫颈黏膜与肌层之间的T2WI低信号间质环用于判断是否累及宫颈肌层，癌前病变组仅1例aLEGH（2.7%）出现低信号间质环中断， G-EAC组低信号间质环中断或消失达46例（86.8%）。与LEGH及aLEGH组相比，G-EAC组多见子宫内膜或肌层累及（34/53，64.2%），且淋巴结增大、宫腔积液和膀胱侵犯只见于G-EAC组。

经单因素分析，病灶范围、大小、成分、增强程度、宫颈间质环、子宫内膜累及、淋巴结增大、宫腔积液在两组间差异有统计学意义（$P<0.05$）；卵巢病变和膀胱侵犯在两组间差异无统计学意义（$P>0.05$）。将单因素分析差异有统计学意义且在两组间均有观察到的特征，进行多因素logistic回归分析，可作为G-EAC显著预测特征的是病灶含实性成分（OR=50.064，95% CI：3.960~632.895）和宫颈间质环不完整（OR=40.180，95% CI：2.961~545.167）。为进一步验证联合上述5个特征对于诊断G-EAC的效能，采用ROC分析结果显示，曲线下面积（area under curve，AUC）为0.970（95% CI：0.931~1.008，图1，表3~5）。

2.3 典型病例

病例1，38岁，否认阴道分泌物增多、不规则出血及腹痛，直肠癌及肠梗阻手术史，个人及家族成员确诊Peutz-Jeghers综合征，宫颈环形电切术后病理学检查证实为LEGH。MRI表现为囊性混合型病灶，即多发大囊、微囊而无明显的实性成分，囊壁光滑，增强后见囊壁明显强化（图2）。

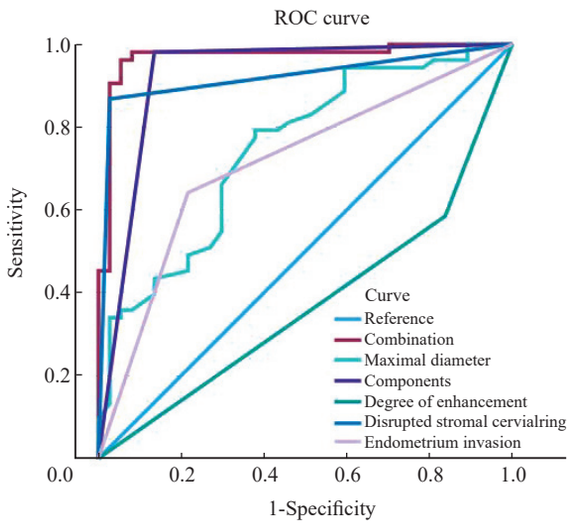

图1 ROC曲线

Fig. 1 ROC curve

病例2，44岁，阴道分泌物增多1年余，全子宫切除后病理学检查结果证实为aLEGH。MRI表现为宫颈管内大囊、微囊弥漫分布，以密集微囊为主，呈“波斯菊花型”，即病灶中央为微小囊，周围包绕着大囊，增强后见微囊呈蜂窝状强化，大囊囊壁轻度强化（图3）。

病例3，43岁，阴道分泌物增多1年余，全子宫切除后病理学检查结果证实为G-EAC。MRI表现为囊实性病灶弥漫分布，累及宫颈管肌层及子宫内膜，宫颈管低信号间质环消失，增强扫描后见实性灶强化程度与子宫肌层相仿，部分囊壁见明显强化（图4）。

表3 宫颈（不典型）叶状增生与胃型腺癌患者MR特征的比较

Tab. 3 Comparison of MRI features between (atypical) LEGH and G-EAC

MRI features	LEGH+aLEGH (n=37)	G-EAC (n=53)	P value
Extent of lesions			
Epithelial layer	37 (100.0%)	11 (20.8%)	<0.001
Muscular layer	0 (0.0%)	42 (79.2%)	
Mean diameter[a]/cm	3.4 ± 1.1	4.7 ± 1.6	<0.001
Components			
Mixed cystic pattern	19 (51.4%)	1 (1.9%)	<0.001
Microcystic pattern	13 (35.1%)	0 (0.0%)	
Mixed cystic-solid pattern	5 (13.5%)	16 (30.2%)	
Solid pattern	0 (0.0%)	36 (67.9%)	
Degree of enhancement			
Mild/moderate	6 (16.2%)	22 (41.5%)	0.011
Significant	31 (83.8%)	31 (58.5%)	
Disrupted cervical stromal ring	1 (2.7%)	46 (86.8%)	<0.001
Endometrium invasion	8 (21.6%)	34 (64.2%)	<0.001
Ovarian lesions	7 (18.9%)	7 (13.2%)	0.462
Lymph nodes enlargement	0 (0.0%)	9 (17.0%)	0.022
Hydrohystera	0 (0.0%)	11 (20.8%)	0.009
Bladder invasion	0 (0.0%)	5 (9.4%)	0.146

[a]: This study measured the maximal diameter of lesions. LEGH: Lobular endocervical glandular hyperplasia; aLEGH: Atypical lobular endocervical glandular hyperplasia; G-EAC: Gastric-type endocervical adenocarcinoma; OR: Odds ratio; CI: Confidence interval.

表4 影像特征的logistic回归

Tab. 4 Logistic regression of MRI features

MRI features	β	SE	Wald test	OR (95% CI)	*P* value
Maximal diameter	−0.141	0.379	0.138	0.868 (0.413-1.827)	0.710
Components	3.913	1.294	9.140	50.064 (3.960-632.895)	0.003
Degree of enhancement	−0.951	1.055	0.813	0.386 (0.049-3.053)	0.367
Disrupted cervical stromal ring	3.693	1.330	7.706	40.180 (2.961-545.167)	0.006
Endometrium invasion	−0.222	1.188	0.035	0.801 (0.078-8.214)	0.852
Constant	−2.262	1.666	1.843	0.104	0.175

表5 影像特征的ROC分析

Tab. 5 ROC analysis of MRI features

MRI features	AUC	SE	Asymptotic Sig.	95% CI
Combination	0.970	0.020	0.000	0.931-1.008
Maximal diameter	0.747	0.052	0.000	0.644-0.849
Components	0.923	0.035	0.000	0.854-0.992
Degree of enhancement	0.374	0.059	0.032	0.258-0.489
Disrupted cervical stromal ring	0.920	0.032	0.000	0.858-0.983
Endometrium invasion	0.713	0.056	0.000	0.604-0.822

AUC: Area under curve; SE: Standard error; Sig.: Significance; CI: Confidence interval.

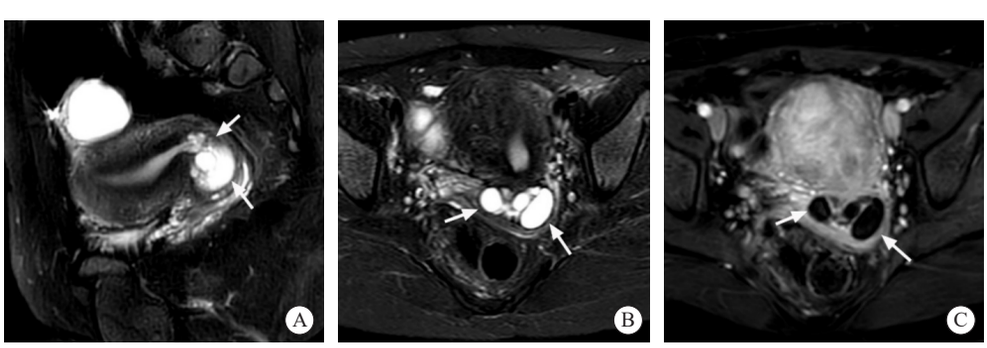

图2 LEGH患者的MRI影像学表现

Fig. 2 MRI features of a LEGH patient

Sagittal (A) and axial (B) T2WI with fat saturation (FS) showed multiple macrocysts and microcysts with smooth cystic walls in the middle and upper endocervical canal (arrows). Axial contrast-enhanced T1WI with FS (C) showed the cystic walls were significantly enhanced, with no obvious solid component.

病例4，51岁，阴道不规则出血4个月余，全子宫切除后病理学检查结果证实为G-EAC。MRI表现为宫颈管内实性团块状肿块，累及宫颈管及子宫下段肌层，宫颈管低信号间质环消失，且左侧髂血管旁可见淋巴结增大，增强扫描后实性灶强化程度弱于子宫肌层（图5）。

图3 aLEGH患者的MRI影像学表现

Fig. 3 MRI features of a aLEGH patient

Axial (A) and sagittal (B) T2WI with FS showed "cosmos pattern" , which was defined as dense microcysts in the center of the lesions surrounded by macrocysts (arrows showed). Sagittal contrast-enhanced T1WI with FS (C) showed dense microcysts with honeycombed enhancement and the walls of macrocysts with mild enhancement.

图4 G–EAC患者病例4的MRI影像学表现

Fig. 4 MRI features of the G-EAC patient case No. 4

Axial (A) and sagittal (B) T2WI with FS showed diffused cystic and solid lesions involving the endometrium and myometrium (arrows) and the cervical stromal ring was missing. Sagittal contrast-enhanced T1WI with FS (C) showed the solid lesions were similar to the enhancement of myometrium and part of cystic walls were significantly enhanced.

图5 G–EAC患者病例5的MRI影像学表现

Fig. 5 MRI features of the G-EAC patient case No. 5

Axial (A) and sagittal (B) T2WI with FS showed a solid mass in the endocervical canal (star) involving the endometrium and myometrium and the cervical stromal ring was missing. Enlarged lymph nodes can be seen adjacent to the left iliac vessels (arrow showed). Sagittal contrast-enhanced T1WI with FS (C) showed the solid lesions were mildly enhanced.

3 讨 论

宫颈癌最常见的病理学类型为鳞状细胞癌和腺癌，可分为人乳头状瘤病毒（human papilloma virus，HPV）相关或非HPV相关性宫颈癌。宫颈鳞癌约占宫颈癌的75%[8]，大多由HPV持续感染引起，根据阴道不规则出血等典型临床表现和宫颈三阶梯检查，一般较易诊断。而G-EAC病因尚不明确，是非HPV相关性子宫颈腺癌中最常

见的一类亚型，其发生率具有明显的地域分布差异，欧美国家宫颈腺癌占比约为10%[9]，而中国占比约为16%[10]。此外，G-EAC临床表现不典型，病灶隐匿而取材困难，筛查和活检阳性率均较低，加之形态学特征与良性病变相似，而生物学特性为高度恶性，给诊治带来极大挑战。

有研究[11-12]报道，可通过MRI最早发现的是宫颈癌病灶ⅠB期病灶，表现为宫颈内局灶性T2WI稍高信号，与正常纤维间质的低信号不同，且MRI病灶的测量值与手术标本的病理学测量值误差＜5 mm，准确率为83%～93%[13]，体现了MRI在诊断宫颈癌中的价值。目前，《子宫颈胃型腺癌临床诊治中国专家共识（2023年版）》[14]认为MRI是术前诊断和评估的首选影像学检查方法。

G-EAC是具有胃型分化的黏液腺癌，类似幽门腺上皮的形态学特征，其组织学表现为腺体的大量增生，患者中位发病年龄约为49岁，故临床上主要表现为阴道分泌物增多，可伴不规则出血和腹痛。LEGH是宫颈上皮分泌细胞组成的腺体良性增生性病变，无核异型性和间质浸润[7]，多见于宫颈管中上段，范围局限，好发于育龄期女性，常见临床表现为大量水样白带。已有研究[2]表明，一定比例的LEGH可恶变为G-EAC，且可共存，因此其被视为癌前病变。本研究中的37例LEGH/aLEGH组和53例G-EAC组患者平均年龄分别为（41.0±10.5）岁和（46.0±12.0）岁，阴道分泌物增多是两组中最常见的症状（52/90，57.8%），而G-EAC组中，有27例（50.9%）出现阴道不规则出血和11例（20.8%）腹痛，上述结果与G-EAC的临床特征一致。

影像学上，LEGH和G-EAC均可呈宫颈多囊性占位，其MRI也存在一定的重叠征象，术前精准诊断及鉴别仍较为困难[15-16]。一般以实性成分为主的G-EAC其MRI良恶性诊断明确，较少发生误诊，而癌前病变和以囊性成分为主的G-EAC则较难以鉴别，易出现过度诊治或漏诊、误诊等情况。本研究中，G-EAC组的术前MRI诊断准确率为79.2%（42/53），仍有20.7%的G-EAC（11/53）被漏诊，而在癌前病变组中MRI术前准确率仅为51.4%（19/37）。Omori等[17]通过MRI将宫颈多囊病变分为花型和树莓型，分别代表许多小囊被大囊包绕和许多密集的微囊，发现树莓型见于绝经妇女可能与LEGH恶变相关。Yoshino等[6]通过MRI先将宫颈病灶成分分为微囊型（≤3 mm），大囊型（＞3 mm），大小囊混合型及囊实性型；进而根据分布形态分为“波斯菊花型”、弥漫型和局灶肿块型；最后综合病灶的位置、成分、形态等将其恶性潜能分为类型1（良性，非LEGH）、类型2（良性，LEGH可能）、类型3（恶性，癌变前或癌可能）和类型4（恶性，癌明确）。其中类型3及4诊断恶性的灵敏度和特异度分别约为61.1%和96.7%。与既往研究[6，16]一致，本研究也认为病灶含实性成分可高度提示恶性（52/53，98.1%），而“波斯菊花型”则更可能提示LEGH。在此基础上，本研究不仅观察了病灶的成分，也进一步评估了其范围、大小、强化程度、宫颈间质环及邻近组织脏器。结果显示，G-EAC的影像学征象更具侵袭性，表现为大多累及宫颈肌层（42/53，79.2%）、子宫内膜（35/53，67.9%），多见宫旁浸润，宫颈间质环常中断消失（46/53，86.8%），病灶更大平均可至（4.7±1.6）cm，上述征象在G-EAC与癌前病变组间差异有统计学意义；晚期患者中还可能观察到宫腔积液、淋巴结增大和膀胱侵犯。在鉴别G-EAC与LEGH和aLEGH时，病灶含实性成分（OR＝50.064，95% CI：5.4～74.1，AUC＝0.923）和宫颈间质环不完整（OR＝40.180，95% CI：2.961～545.167，AUC＝0.920）有很高的诊断效能，联合观察多个特征有助于鉴别G-EAC。

本研究存在以下局限：首先，采用回顾性分析，入组患者可能存在选择偏移，且各病理学类型的样本量均有待进一步扩大；其次，本研究未对患者的MRI图像进行动态观察比较；最后，可观察的征象有待丰富完善，如尚未对弥散加权成像（diffusion weighted imaging，DWI）序列的表现进行分析比较[18]。

综上所述，本研究重点分析LEGH、aLEGH和G-EAC的影像学特征，提出结合多个MRI征象

可在早期识别和鉴别上述病变，为癌前病变患者密切随访和G-EAC患者早诊早治提供有效的检查手段，进而改善患者预后。未来为进一步提高LEGH与G-EAC的术前鉴别能力，可结合影像学表现、临床表现和实验室检查以建立多维度的诊断模型，从而更有助于临床医师的治疗决策。

利益冲突声明：所有作者均声明不存在利益冲突。

作者贡献声明：

马凤华：提出研究方向、设计研究思路、实施研究过程、修订论文；姜安绮：确定研究对象范围、收集并分析数据、设计论文框架、起草论文；陈奕清：文献调研与整理；徐丛剑：审核论文、修订论文；康玉：参与提出研究方向、修订论文。

［参 考 文 献］

［1］ NUCCI M R, CLEMENT P B, YOUNG R H. Lobular endocervical glandular hyperplasia, not otherwise specified: a clinicopathologic analysis of thirteen cases of a distinctive pseudoneoplastic lesion and comparison with fourteen cases of adenoma malignum［J］. Am J Surg Pathol, 1999, 23(8): 886–891.

［2］ TALIA K L, MCCLUGGAGE W G. The developing spectrum of gastric–type cervical glandular lesions［J］. Pathology, 2018, 50(2): 122–133.

［3］ EHMANN S, SASSINE D, STRAUBHAR A M, et al. Gastric–type adenocarcinoma of the cervix: clinical outcomes and genomic drivers［J］. Gynecol Oncol, 2022, 167(3): 458–466.

［4］ TAKATSU A, SHIOZAWA T, MIYAMOTO T, et al. Preoperative differential diagnosis of minimal deviation adenocarcinoma and lobular endocervical glandular hyperplasia of the uterine cervix: a multicenter study of clinicopathology and magnetic resonance imaging findings［J］. Int J Gynecol Cancer, 2011, 21(7): 1287–1296.

［5］ TSUBOYAMA T, YAMAMOTO K, NAKAI G, et al. A case of gastric–type adenocarcinoma of the uterine cervix associated with lobular endocervical glandular hyperplasia: radiologic–pathologic correlation［J］. Abdom Imaging, 2015, 40(3): 459–465.

［6］ YOSHINO A, KOBAYASHI E, TSUBOYAMA T, et al. Novel strategy for the management of cervical multicystic diseases［J］. Ann Surg Oncol, 2023, 30(5): 2964–2973.

［7］ KOBARA H, MIYAMOTO T, ANDO H, et al. Limited frequency of malignant change in lobular endocervical glandular hyperplasia［J］. Int J Gynecol Cancer, 2020, 30(10): 1480–1487.

［8］ NOSÉ V, LAZAR A. Update from the 5th edition of the World Health Organization classification of head and neck tumors: familial tumor syndromes［J］. Head Neck Pathol, 2022, 16: 143–157.

［9］ STOLNICU S, BARSAN I, HOANG L, et al. International endocervical adenocarcinoma criteria and classification (IECC): a new pathogenetic classification for invasive adenocarcinomas of the endocervix［J］. Am J Surg Pathol, 2018, 42(2): 214–226.

［10］ 吕炳建, 石海燕, 邵 颖, 等. 基于国际颈管腺癌标准与分类286例宫颈腺癌临床病理与预后分析［J］. 中华病理学杂志, 2021, 50(9): 1014–1019.
LÜ B J, SHI H Y, SHAO Y, et al. Endocervical adenocarcinomas classified by International Endocervical Adenocarcinoma Criteria and Classification: a clinicopathological and prognostic analysis of 286 cases［J］. Chin J Pathol, 2021, 50(9): 1014–1019.

［11］ SALIB M Y, RUSSELL J H B, STEWART V R, et al. 2018 FIGO staging classification for cervical cancer: added benefits of imaging［J］. Radiographics, 2020, 40(6): 1807–1822.

［12］ XIAO M L, YAN B C, LI Y, et al. Diagnostic performance of MR imaging in evaluating prognostic factors in patients with cervical cancer: a meta–analysis［J］. Eur Radiol, 2020, 30(3): 1405–1418.

［13］ SALEH M, VIRARKAR M, JAVADI S, et al. Cervical cancer: 2018 revised international federation of gynecology and obstetrics staging system and the role of imaging［J］. AJR Am J Roentgenol, 2020, 214(5): 1182–1195.

［14］ 中国医师协会妇产科医师分会妇科肿瘤学组. 子宫颈胃型腺癌临床诊治中国专家共识(2023年版)［J］. 中国实用妇科与产科杂志, 2023, 39(6): 617–625.
Gynecologic Oncology Group of Chinese Association of Obstetricians and Gynecologists. Chinese expert consensus on clinical diagnosis and treatment of gastric–type endocervical adenocarcinoma (2023 edition)［J］. Chin J Pract Gynecol Obstet, 2023, 39(6): 617–625.

［15］ STOEHR A, NANN D, STAEBLER A, et al. Difficulties in diagnosis of a minimal deviation adenocarcinoma of uterine cervix diagnosed postoperatively: brief communication and literature review［J］. Arch Gynecol Obstet, 2019, 300(4): 1029–1043.

［16］ SAIDA T, SAKATA A, TANAKA Y O, et al. Clinical and MRI characteristics of uterine cervical adenocarcinoma: its variants and mimics［J］. Korean J Radiol, 2019, 20(3): 364–377.

［17］ OMORI M, KONDO T, TAGAYA H, et al. Utility of imaging modalities for predicting carcinogenesis in lobular endocervical glandular hyperplasia［J］. PLoS One, 2019, 14(8): e0221088.

［18］ SCHREUDER S M, LENSING R, STOKER J, et al. Monitoring treatment response in patients undergoing chemoradiotherapy for locally advanced uterine cervical cancer by additional diffusion–weighted imaging: a systematic review［J］. J Magn Reson Imaging, 2015, 42(3): 572–594.

（收稿日期：2023-12-29 修回日期：2024-04-03）